FORUM GEOGRAFI
ISSN: 0852-0682 | E-ISSN: 2460-3945
HTTPS://JOURNALS.UMS.AC.ID/INDEX.PHP/FG/

Research article

Impact of Climate Change on the Cryosphere of the Ugam Chatkal National Park, Bostonliq District, Uzbekistan, During the Post-Soviet Period, Based on Remote Sensing and Statistical Analysis

Bokhir Alikhanov[1,*], Bakhtiyor Pulatov[1], Luqmon Samiev[1,2]

[1] Research Institute of Environment and Nature Conservation Technologies, Ministry of Ecology, Environmental protection and Climate change, Tashkent 100043, Uzbekistan
[2] Tashkent Institute of Irrigation and Agricultural Mechanization Engineers, National Research University, Tashkent 100000, Uzbekistan

[*)] Correspondence: alihanovbahir@gmail.com

Citation:
Alikhanov, B., Pulatov, B., & Samiev, L. (2024). Impact of Climate Change on the Cryosphere of the Ugam Chatkal National Park, Bostonliq District, Uzbekistan, During the Post-Soviet Period, Based on Remote Sensing and Statistical Analysis. Forum Geografi. 38(3), 302-316.

Article history:
Received: 24 February 2024
Revised: 11 June 2024
Accepted: 15 July 2024
Published: 13 September 2024

Abstract

The cryosphere, including glaciers, snow cover, and ice sheets, plays a crucial role in global climate regulation. Therefore, monitoring is crucial for understanding climate dynamics at both regional and global scales. According to scientists studying global climate change, Central Asia is vulnerable to global temperature increases. However, research aimed at analyzing the impact of climate change on the regional cryosphere is lacking. This study investigated the impact of climate change on the cryosphere of the Ugam Chatkal National Park in Uzbekistan's Bostonliq District, focusing on the period following the dissolution of the Soviet Union (1991–2022). This study used remote sensing data and statistical analyses, such as the Mann–Kendall test and Sen's slope calculations, to evaluate trends in snow and ice cover, glacier extent, and vegetation health. Key indices, such as normalized difference vegetation index, normalized difference snow index, normalized difference glacier index, and normalized difference snow-ice index, were used to measure the mean values of these environmental parameters. The findings indicate a significant decrease in snow/ice cover (slope =-0.0048, tau =-0.193), underscoring the profound effects of climate warming on the region's water resources and ecological balance. The analysis highlights the urgency of implementing adaptive management strategies to mitigate these impacts, ensure the sustainability of water supply, and preserve biodiversity in Central Asia's vulnerable mountain ecosystems.

Keywords: cryosphere; Uzbekistan; NDSI; remote sensing; climate change.

1. Introduction

The evolving state of the cryosphere is an indicator of global warming. Alterations in snow cover, glaciers, and permafrost serve as indicators of shifts in atmospheric conditions and sea-level rise, underscoring ongoing changes in the environment (Gardner *et al.,* 2013; Nüsser *et al.,* 2017). In recent years, these transformations have substantially impacted the principal mountain ranges of Central Asia, namely Tien Shan and Pamir (Barandun *et al.,* 2020). Permafrost exhibits considerable variation in ice content based on the underlying material, such as rock glaciers, bedrock, and fine sediments. For instance, a rock glacier's ice content can range from 10 to 90% by volume, whereas massive bedrock typically contains minimal ice. Although such varied permafrost landforms exist in the highlands of Central Asia, their specific quantities have not been thoroughly measured (Barandun *et al.,* 2020; Zhang *et al.,* 2013).

Snow accumulation is crucial for water storage, primarily during winter, and significantly influences river runoff in spring and early summer. The summer precipitation increases towards the east, leading to frequent summer snowfall. Snow has a profound effect on the ground temperature regime, thereby affecting the distribution of permafrost. In addition, fresh snowfall increases the albedo effect, leading to a marked decrease in glacier melting. Glaciers and permafrost typically release most meltwater between July and September. During times of drought and high temperatures, glacial melt becomes an essential source of freshwater. However, the contribution of permafrost melt to the overall river runoff remains unclear (Barandun *et al.,* 2020; Kenner *et al.,* 2019; Shahgedanova *et al.,* 2018).

Snow cover, glaciers, permafrost, and ice caps are distinct features of Earth's cryosphere, each with unique characteristics and impacts on the global climate system and water cycle. A brief overview of each snow cover type refers to the layer of snow that accumulates on the ground in cold environments and during winter in temperate regions (Gascoin *et al.,* 2020). It can vary in depth and duration, markedly affecting local temperature, soil moisture, and ecosystems. Snow acts as a temporary water store, releasing water during its melting phase, and glaciers are large, persistent bodies of dense ice that form over centuries from accumulated snowfall and its compaction into ice. They are found in mountainous regions and polar areas (Singh *et al.,* 2011). Glaciers move slowly over land because of their weight, shaping the landscape through erosion.

They serve as long-term reservoirs of freshwater, but are sensitive indicators of climate change, with their retreat signalling global warming. Glaciers, which are large and frozen masses of ice, play a significant role in the Earth's climate. They are highly reflective surfaces, implying that they bounce a large portion of the sunlight that hits them back into the atmosphere, a process known as the albedo effect (Hill *et al.,* 2017; Mohammadi *et al.,* 2023), while permafrost is the ground (soil or rock, including ice or organic material) that remains completely frozen for 2 or more consecutive years. It is found in high-latitude regions (such as the Arctic) and at high elevations in the mountains. Permafrost affects soil processes, vegetation, and the construction of buildings and roads. Thawing permafrost due to climate change releases greenhouse gases such as methane and carbon dioxide, exacerbating global warming (Haeberli, 2004). The differences between ice, snow, glaciers, and permafrost are listed in Table 1.

Table 1. Comparison between cryosphere components.

Feature	Ice	Snow	Glaciers	Permafrost
State of matter	Solid	Solid (partially melted)	Solid	Solid
Formation	Freezing of water	Precipitation and re-freezing	Compaction and transformation of snow	Freezing of ground below 0 °C for 2 or more consecutive years
Properties	Hard, rigid, transparent/translucent	Fragile, porous, opaque white	Large, moving, exhibit features	Permanently frozen ground may contain ice, water, and organic matter
Examples	Ice cubes, sea ice	Fresh snowfall, snow-pack	Mountain glaciers, ice sheets	Arctic tundra, high mountain slopes

Glaciers in Central Asia serve as vital, long-standing freshwater reserves that release water during peak demand times in hot months, which are crucial for irrigation. Their sensitivity to rising temperatures implies that they are notably affected by climate change, which in turn impacts the flow of glacier-fed rivers, with immediate consequences for freshwater availability, irrigation, and hydropower production. Consequently, glacier shrinkage threatens sustainable development as well as energy and food security in the region (Diebold, 2013). Central Asia faces challenges in reconciling environmental conservation with the demand for hydropower and agriculture. This situation has been exemplified by the desiccation of the Aral Sea over the past five decades. Countries upstream of the Aral Sea Basin, such as Kyrgyzstan, Tajikistan, and Afghanistan, prioritize water for winter hydropower generation, whereas downstream nations, such as Uzbekistan, Kazakhstan, and Turkmenistan, require water for irrigation during the growing season, leading to conflicting interests (Barandun *et al.,* 2020; Diebold, 2013).

Ice and snowmelt serve as key water sources for the densely populated lowlands of the region and play vital roles in supporting both the region and the mountain communities. In areas where irrigation is widely practiced, ongoing interactions between society and hydrology have been established, highlighting the critical importance of natural water resources for sustaining agricultural and community livelihoods (Mohammadi *et al.,* 2023; Nüsser, 2017). Glaciers are widely regarded as key indicators of climate change and serve as sensitive and valuable elements for observing swift responses to climate change. Their dynamics, including their rates of melting and retreat, provide clear evidence of changes in global and regional temperatures, making them critical tools for climate scientists studying the impacts of environmental change (Florath *et al.,* 2022; Gul *et al.,* 2020).

Cryosphere alterations caused by climate change have a marked impact on the frequency and intensity of natural hazards. As glaciers and permafrost degrade, the hazards associated with these changes are anticipated to occur more often and with greater force (Gul *et al.,* 2020). The processes triggered by this degradation have the potential to affect densely populated regions, extend across national borders, and cause numerous casualties. This highlights the growing concern over the direct and indirect effects of climate warming on natural disaster risks, and emphasizes the need for preparedness and mitigation efforts in vulnerable areas (Barandun *et al.,* 2020; Stoffel & Huggel, 2012).

Simultaneously, the gradual thawing of permafrost can trigger significant geological events, in-including large rockfalls. These events can set off a series of cascading disasters involving processes such as the overtopping of natural or artificial dams and breaches in lake dams. Such breaches can lead to massive debris flows (Frolov *et al.,* 2023). These flows are swift-moving and highly destructive masses of rock, earth, and water that sweep down mountainous areas and pose serious threats to life, infrastructure, and the environment in their path. The potential for such cascading events underscores the complex and interconnected risks posed by permafrost

degradation in a warming climate, highlighting the need for comprehensive risk assessments and management strategies in vulnerable regions (Worni *et al.,* 2014).

Remote sensing is a pivotal tool for cryospheric analysis. The ability to monitor these elements in space using satellite imagery provides invaluable data for understanding climate change and its impacts. For instance, satellite missions, such as NASA's Landsat and the European Space Agency's Sentinel-1 and Sentinel-2, offer high-resolution images that enable detailed mapping and monitoring of glacial movements and changes in ice extent (National Snow & Ice Data Center, 2024). The use of synthetic aperture radar (SAR) from satellites, such as Sentinel-1, is particularly effective for penetrating cloud cover and darkness, allowing for year-round observations of ice dynamics (Xiong *et al.,* 2020).

One notable application of remote sensing in cryosphere analysis is the monitoring of the Greenland and Antarctic ice sheets. Studies utilizing data from the Gravity Recovery and Climate Experiment (GRACE) satellites have quantified significant ice mass loss in these regions, contributing to global sea level rise (Velicogna & Wahr, 2013). Additionally, remote sensing technologies such as the Moderate Resolution Imaging Spectroradiometer (MODIS) have been instrumental in tracking changes in snow cover extent and duration across various mountain ranges, which are crucial for water resource management in several parts of the world (Hall & Riggs, 2011). These examples highlight the critical role of remote sensing in advancing our understanding of cryospheric processes and their broad environmental implications.

Studies conducted within the Oygaing River Basin in Uzbekistan have verified the ongoing shrinkage of glaciers. During 1957–1978, the glacier area in this basin experienced a reduction of 10%, and the trend worsened from 1978 to 2001, with a decline of 16%. The Center for Hydrometeorology of the Cabinet of Ministers of the Republic of Uzbekistan (Uzhydromet) is tasked with monitoring the surge of glacial lakes, which are key indicators of glacial retreat. These lakes pose a risk because of their relatively unstable moraines, which often have an ice-cold core. If the meltwater exceeds the drainage capacity of the lake, the pressure increases, increasing the risk of sudden outbursts. These events can cause significant damage and loss of life. Therefore, monitor- ing glaciers and moraine lakes is crucial to provide advance warnings of potential outbursts (Diebold, 2013).

A recent study by Alikhanov *et al*. (2021) used machine learning algorithms (namely random forests and CA-Markov) to detect land cover change in Ugam Chatkal National Park from 1991 to 2022 with Landsat satellite images, as well as predict future scenarios if land cover shifts for the region for the next 40 years. Their study showed a gradual decline in snow cover in mandated areas of the park, and its replacement with rock and vegetation cover. In all three scenarios, the authors predicted the future diminishment of the cryosphere area to different degrees of extent. These findings are also corroborated by a study conducted in the same study area, where the authors analyzed the monthly vegetation cover change (utilising normalized difference vegetation index (NDVI) and SAVI indices) for the 1991–2022 period using the Google Earth Engine and Landsat satellites. The results showed that the area experienced a gradual increase in vegetation during the post-Soviet period of time (Alikhanov et al., 2021). This article continues the sequence of interrelated and interconnected studies aimed at understanding the impact of climate change on land cover shifts in the Ugam Chatkal National Park, Bostonliq district, during the period from 1991 to 2022, which is also known as the post-Soviet era. The goal of this research was to conduct an analysis of the cryosphere change of the Ugam Chatkal National Park, Bostanliq district, Uzbekistan, during the post-Soviet period (1991–2022) using remote sensing indices and the impact of climate on it.

2. Research Methods

2.1. Study area

The Republic of Uzbekistan's terrain is partitioned into two disproportionate segments: approximately three-quarters, or 78.8%, consists of plains, whereas the remaining quarter, or 21.2%, is comprised of mountains and valleys nestled within mountain ranges (Petrov *et al.,* 2017). Approximately 90% of the river water utilized by Uzbekistan originates from rivers that begin in the neighbouring countries (Sorg *et al.,* 2015).

The mountainous region surrounding the capital of Uzbekistan is categorically divided into two main areas: the northeastern part encompasses the Chirchik River Basin and the southeastern section includes the Angren region within the Akhangaran River Basin. This area incorporates the river basins of Pskem, Chatkal, Oygaing, Ko'ksuv, and Angren. Situated in the northeastern portion of Uzbekistan, it lies between the Syr Darya River and extensions of the Western Tien

Shan Mountains. The Chirchik-Akhangaran district extends longitudinally from the northeast to the southwest over 280 km and spans 180 km from east to west (Alikhanov *et al.,* 2021; Petrov *et al.,* 2017).

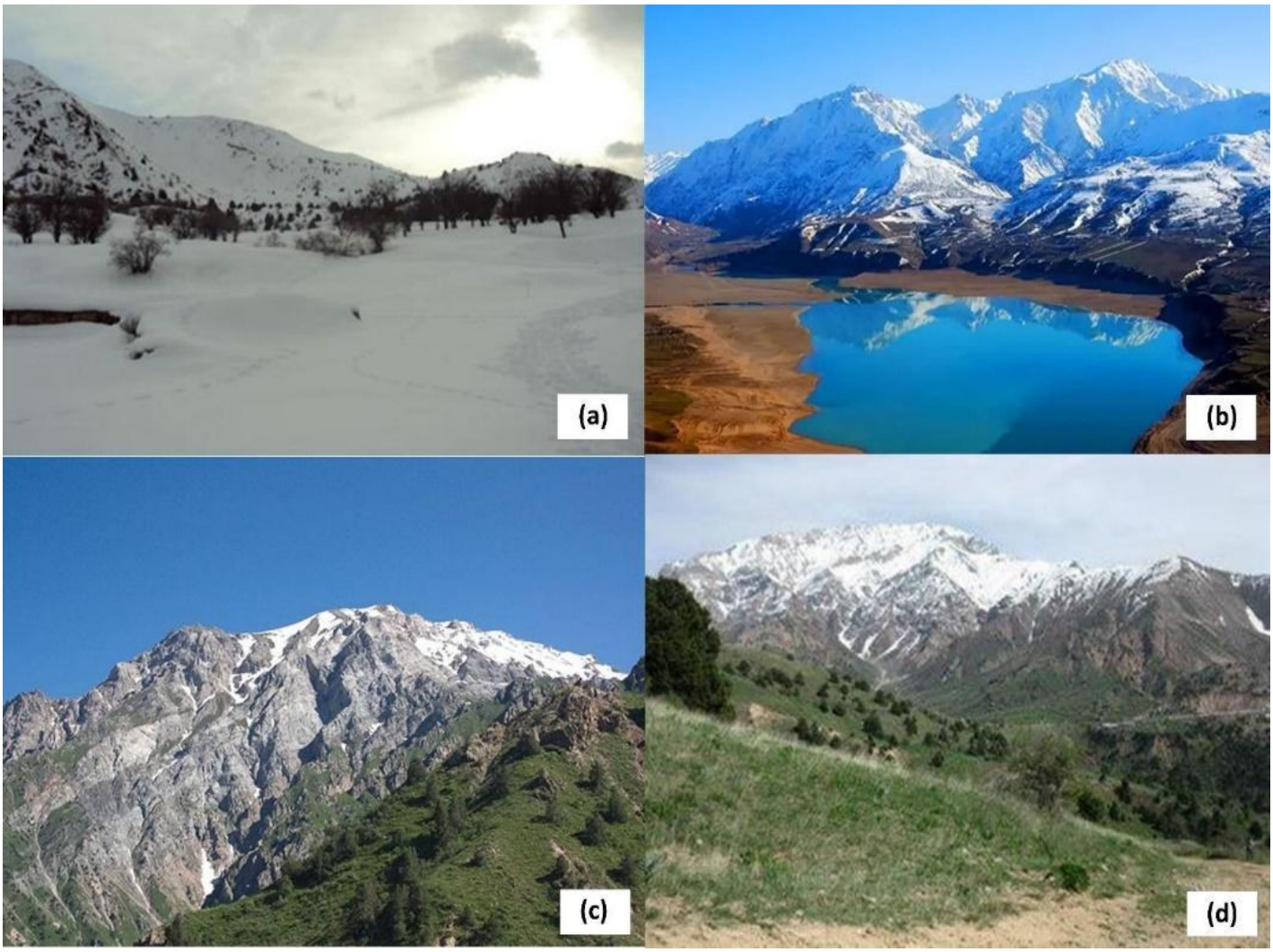

Figure 1. Chatkal Mountain Range (part of Eastern Tian Shian) covers the north of Bostanliq district with the Chimgan mountain being the tallest and largest of all mountains. The autumn and winter periods are covered with snow and glaciers (a and b), with complete melting of snow cover and reduction of glacier cover starting in late spring until September (c and d).

The topography of the Chirchik and Akhangaran districts is complex. The terrain slopes downward from the northeast to the southwest towards the Syr Darya River, with the highest points found in the northeastern and eastern sections of the region. In contrast, it is relatively high in the southwestern area. This region has experienced a high rate of tectonic activity, which contributed to its complex relief. The apex of the Chirchik-Akhangaran district is Mount Beshtor, which reaches an elevation of 4,299 meters (Petrov *et al.,* 2017). In the mountainous region, the average summer temperature is around 20°C. During the winter, the coldest temperatures can plummet to as low as −30 °C. The plains receive 250–300 mm of precipitation annually. In the foothill areas, precipitation increases to 350–400 mm. The western part of the mountains, which encounters cold air masses, experiences significantly higher precipitation levels ranging from 800 to 900 mm.

The Chirchik River Basin, covering an area of 14,900 km^2, is replenished by meltwater from the Chatkal and Pskem Rivers. The Chatkal River originates from the southwestern slopes of Talas Alatau and flows westward, tracing the westernmost part of the Tien Shan mountain range, with Sandalash to its north and Koksu-Chatkal to its south. The source of the Pskem River can be traced back to the glaciers of the Talas Alatau, spanning Kazakhstan and Uzbekistan (Alikhanov *et al*., 2020; Petrov *et al.,* 2017). The Akhangaran River, with a catchment area of 7,710 km^2, is the second-largest river in the Tashkent region. It springs from the Chatkal range, and its entire basin is situated within the Republic of Uzbekistan. As a tributary of the Syr-Darya River, the Akhangaran River exhibits peak discharge levels in April and May (Petrov *et al.,* 2017).

Throughout autumn and winter, snow and glaciers create blank landscapes. However, in late spring, snow began to melt extensively, and glacier coverage dwindled steadily until September (Figure 1).

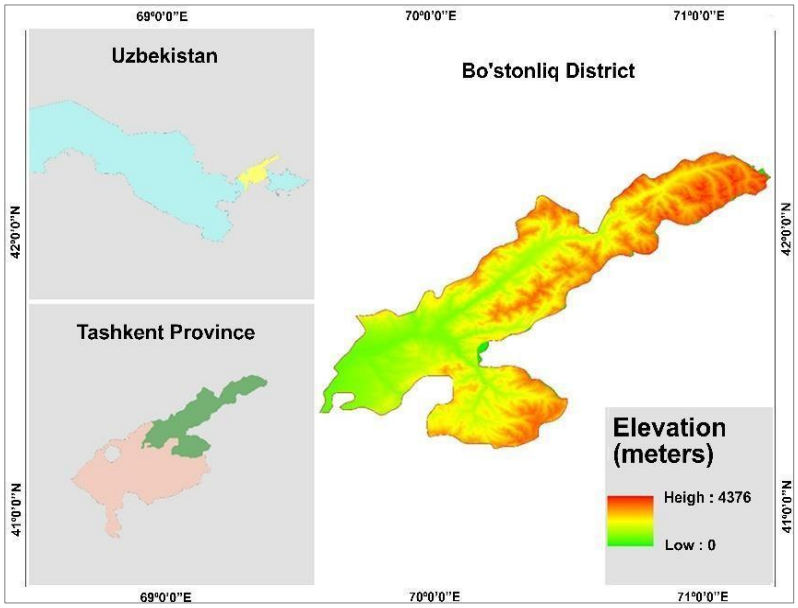

Figure 2. Approximately 90% of Ugam Chatkal National Park area is located in the Bostonliq district.

2.2. Data

Both remote sensing and meteorological data were used in this study. Remote sensing data, namely satellite data, were analysed using the Google Earth Engine platform. We used Landsat 5 TM, Landsat 7 ETM, and Landsat 8 OLI satellites atmospherically corrected images, with a cloud cover maximum of 8%. In general, 235 images (26 images from Landsat 5 TM, 114 images from Landsat 7 ETM, and 95 images from Landsat 8 OLI) were analysed using cryosphere indices. However, very few images were available for the period of 1991–2000 (Landsat 5), which reduced the robustness of this research. To comprehensively analyse each image, we extracted different statistical parameters, such as the mean, median, minimum, and maximum. The temporal resolution (revisit time) of all three satellites was 16 days.

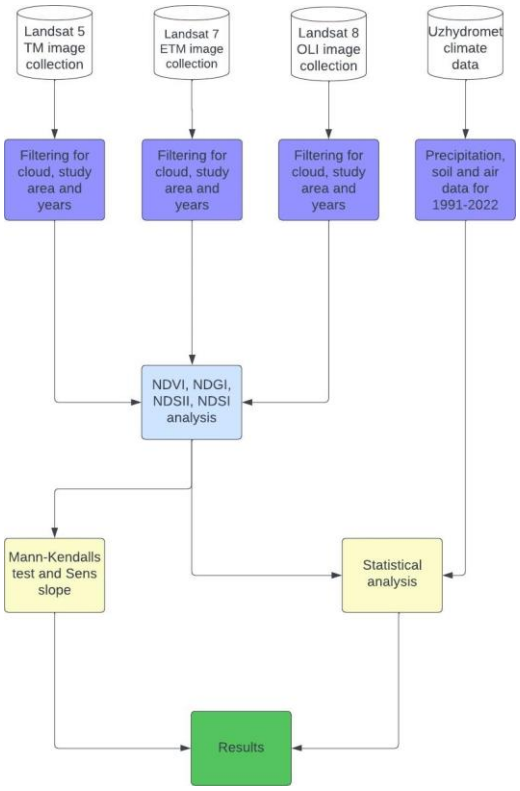

Figure 3. Flow chart of the cryosphere analysis.

Meteorological data spanning three decades (1991–2022) were obtained from the Agency of Hydrometeorological Services, which operates under the Ministry of Ecology, Environmental Protection, and Climate Change of the Republic of Uzbekistan (Uzhydromet). This data collection purposefully focused on variables that are closely linked to land cover and climatic conditions, specifically total monthly precipitation, average monthly temperature, and average monthly soil temperature (Figure 3).

Combined, these data were comprehensively analysed using the Mann–Kendall (MK) test and Sen's slope for long-term trend direction and magnitude and for correlation and regression relationships between each other using Pearson's correlation.

2.3. Remote sensing analysis of the cryosphere

Owing to its importance in water security and climate balance, in recent decades, constant and scrupulous monitoring and assessment of cryosphere components (such as ice, snow, and glaciers) using remote sensing have become very popular (Robson *et al.,* 2020).

Hall et al. (1995) introduced the normalised difference snow index (NDSI), a method aimed at identifying areas covered by snow (Hall *et al.,* 1995). This index detects snow cover using green and short-wave infrared reflectance bands (Equation 1).

$$NDSI = \frac{Green - SWIR}{Green + SWIR} \quad (1)$$

Pixels with values from 0.4 and higher are considered snow cover (Hall *et al.,* 1995). However, water bodies also have a high NDSI; therefore, an increase in the index of the study area does not necessarily imply an increase in snow cover if the water body changes throughout the period.

The use of the NDSI for glacier mapping has certain limitations. For example, this index might struggle to differentiate between snow and ice or accurately identify pixels that represent water (Mohammadi *et al.,* 2023). Previous research has highlighted various critical shortcomings of the NDSI in snow and glacial mapping.

These include challenges in distinguishing snow/glacier pixels from background pixels, misclassification of water pixels as snow or glacier pixels, and inconsistencies in the threshold values for the NDSI across different geographical regions (Choubin *et al.,* 2019; Sood *et al.,* 2020).

Mohammadi *et al.* (2023) developed an adjusted normalised snow difference index (ANDSI), compared it with the NDSI, and compared it to four countries (Sweden, Canada, Switzerland, and China) for mapping glaciers. The results showed that the newly developed index yielded slightly better results than the older index. (Wang *et al.,* 2017) used the NDSI for glacial mapping of Landsat 8 images in the eastern Karakorum Mountain system. These findings indicate that the NDSI method is effective in delineating the most defined glacial boundaries and capturing high-resolution imagery of small-scale glacier features. However, this technique falls short in differentiating between glaciers and lakes, highlighting a limitation in its ability to accurately classify distinct water bodies (He *et al.,* 2020).

Keshri *et al.* (2009) discovered notable differences between snow, ice, and glacier cover while researching the Chenab Basin in the Himalayas using ASTER satellite images. As a result of the investigation and differentiation among the snow, ice, snow-ice debris, and glaciers, two new indices were developed by the authors: the normalised difference glacier index (NDGI), Equation 2.

$$NDGI = \frac{Green - SWIR}{Green + SWIR} \quad (2)$$

and Normalized difference snow-ice index (NDSII) Equation 3.

$$NDSI = \frac{Green - NIR}{Green + NIR} \quad (3)$$

NDVI is the most popular index for detecting vegetation cover using remote sensing because of its simplicity. The principle of the NDVI involves subtracting the red electromagnetic spectrum reflected from the land surface from the near-infrared spectrum (NIR) (Gabban *et al.,* 2004). Healthy vegetation reflects most of the incoming NIR light and absorbs red light. Finding the difference between them and dividing them into the sum of Red and NIR can provide accurate information about the value of the sum of the NIR. Red can provide information about the state

of vegetation on the pixel (high and healthy vegetation, sparse vegetation, absence of vegetation, etc.) (Hussien *et al.,* 2023), Equation 4.

$$NDVI = \frac{NIR - RED}{NIR + Red} \quad (4)$$

2.4. Mann–Kendall test and Sen's slope

The MK test is a nonparametric method employed to identify notable trends within a sequence of data points, such as those related to hydrology and climate, without the prerequisite of a specific distribution for the dataset. This approach recognises trends, although it does not define whether they follow a linear pattern. The MK test is designed to evaluate the null hypothesis, which posits the absence of any trend, against an alternative hypothesis suggesting the existence of a trend. For datasets that are extensive (comprising 50 or more data points) and exhibit a significant trend magnitude (with a slope equal to or greater than 0.01), it is unnecessary to adjust the data for serial correlation through pre-whitening prior to conducting the MK test (Mann, 1945). The test statistic S was determined by comparing each data point within the series against all subsequent data points, Equation 5.

$$S = \sum_{k}^{n} \sum_{k=j+1}^{n} Sgn(y_j - y_k) \quad (5)$$

where n is the total number of data points, yj and yk are the data points at times j and k (j>k), respectively, and Sgn ($\boldsymbol{yj} - \boldsymbol{yk}$) is a function that is calculated as, Equation 6.

$$Sgn(y_j - y_k) = \{1, if\ y_j > y_k\, 0, if\ y_j = y_k - 1, if\ y_j < y_k \quad (6)$$

The Tau (τ) statistic for the Mann-Kendall test is a measure of correlation and is calculated as Equation 7.

$$r \frac{S}{\sqrt{(n(n-1))/2}\sqrt{n(n-1)(2n+5) - \sum ti\,(ti-1)(2ti+5)/18}} \quad (7)$$

Where:

n is the number of data points,

m is the number of tied groups in the data,

tp is the number of data points in the pth-tied group.

The Sen's slope estimator, developed by Pranab Kumar Sen in 1968, is a non-parametric method used to estimate the slope of a trend within a set of data points and is often applied in conjunction with the MK test for trend analysis. It is particularly useful for data that may not follow a normal distribution and is robust against outliers. Sen's slope has been widely used in environmental science, hydrology, and climatology to detect changes in variables over time (Sen, 1968).

For each pair of time-ordered data points (xi,yi) and (xj,yj) where j>i, calculate the slope (θij) as Equation 8.

$$\theta ij = \frac{y_i - y_i}{x_i - x_i} \quad (8)$$

Sen's slope estimator is a tool used to quantify the magnitude of a trend within a dataset. When combined with the MK test, which evaluates the existence of a trend, Sen's slope offers insight into the steepness of the trend. This combination is particularly valuable for the examination of environmental datasets, where understanding trends over time, such as changes in temperature, precipitation, and water quality indicators, is critical. Sen's slope calculates the rate of change between each pair in a data series, providing a numerical value that represents how sharp or gradual the observed trend is. MK and Sen's slope were used to analyse cryosphere indices for trends during the study period. If the tau coefficient is different from zero and the p-value is less than 0.05, the zero hypothesis is rejected, and the alternative hypothesis is confirmed. These methods are more suitable for detecting long-term trends and can be adjusted for data with large variances and gaps.

For environmental data, which often exhibit nonlinear trends and seasonality, and are subject to various external influences, the MK test and Sen's slope can offer a robust methodology for trend analysis without the constraints of the parametric method The MK test effectively detects trends in time-series data without assuming any specific data distribution, making it robust against non-normal distributions often observed in environmental data. This test's resistance to outliers and

ability to handle missing data, which can occur due to the 8% cloud cover in remote sensing observations, make it an ideal choice for our analysis.

Complementing the MK test, Sen's slope estimator provides a robust measure of the magnitude of the trend, unaffected by outliers or the non-normality of the data. This combination offers a reliable way to quantify the rate of change in cryosphere indices such as snow cover extent or glacier area. By applying these methods, we can accurately detect and measure significant trends, thereby enhancing our understanding of seasonal variations and long-term changes in the cryosphere driven by climate change.

3. Results and Discussion

The results of the remote sensing and meteorological data were statistically analysed for longitudinal changes. However, because of the absence of sufficient data from Landsat 5 TM atmospherically corrected images, it was difficult to precisely and robustly examine the first decade of the post-Soviet period in the Bostonliq district. Several abrupt changes were noted in all the indices (NDSI, NDSII, NDVI, and NDGI) throughout the study period (Figure 4). The NDSI index showed the highest values (reaching 0.8 during winter). Most of the area is covered with snow during winter, which starts to melt in March and evaporates until June–July, gradually replacing the snow with vegetation.

NDSII and NDGI showed relatively low values compared with NDSI, both reaching maximum values during the winter period (from 0 to 0.2). Nevertheless, NDSII reached the lowest values (-0.3 to -0.4) during the middle of summer, when other cryosphere indices also dropped to the lowest level, whereas the NDVI reached its peak. The glacier index fluctuated throughout the year but seldom exceeded zero.

Data gaps (particularly in 1992, 1997, and 1999) make it difficult to analyse this period astutely for cryosphere degeneration or regeneration. As predicted, all three cryosphere indices showed the same pattern of change; however, different values were negatively correlated with vegetation cover.

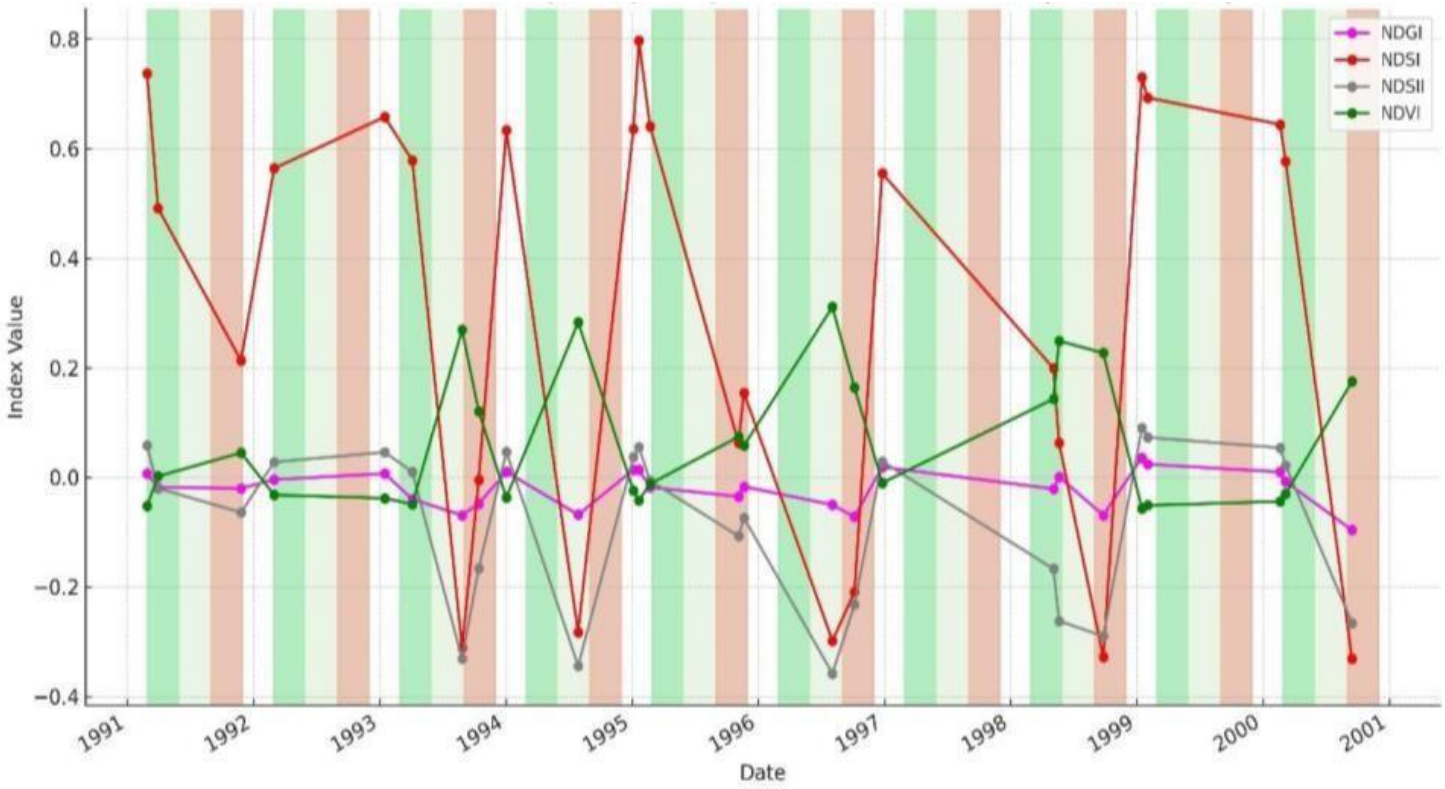

Figure 4. Time-series change of UCHNP cryosphere from 1991 to 2022 using Landsat 5. Different colours show different seasons of the year.

Notably, for the second and beginning of the third decade of the post-Soviet period, sufficient number of images from the Landsat 7 sensor were available, which facilitated a more detailed analysis of the glacier and snow cover changes and differences among indices. The NDSI and NDSII showed similar patterns, with the highest values during January and February and the lowest values during autumn (September and October; Figure 5). The NDGI showed a similar

trend, but the glacier cover started to diminish from April and reached its lowest level in August and September when the NDSII started to recover (Figure 5).

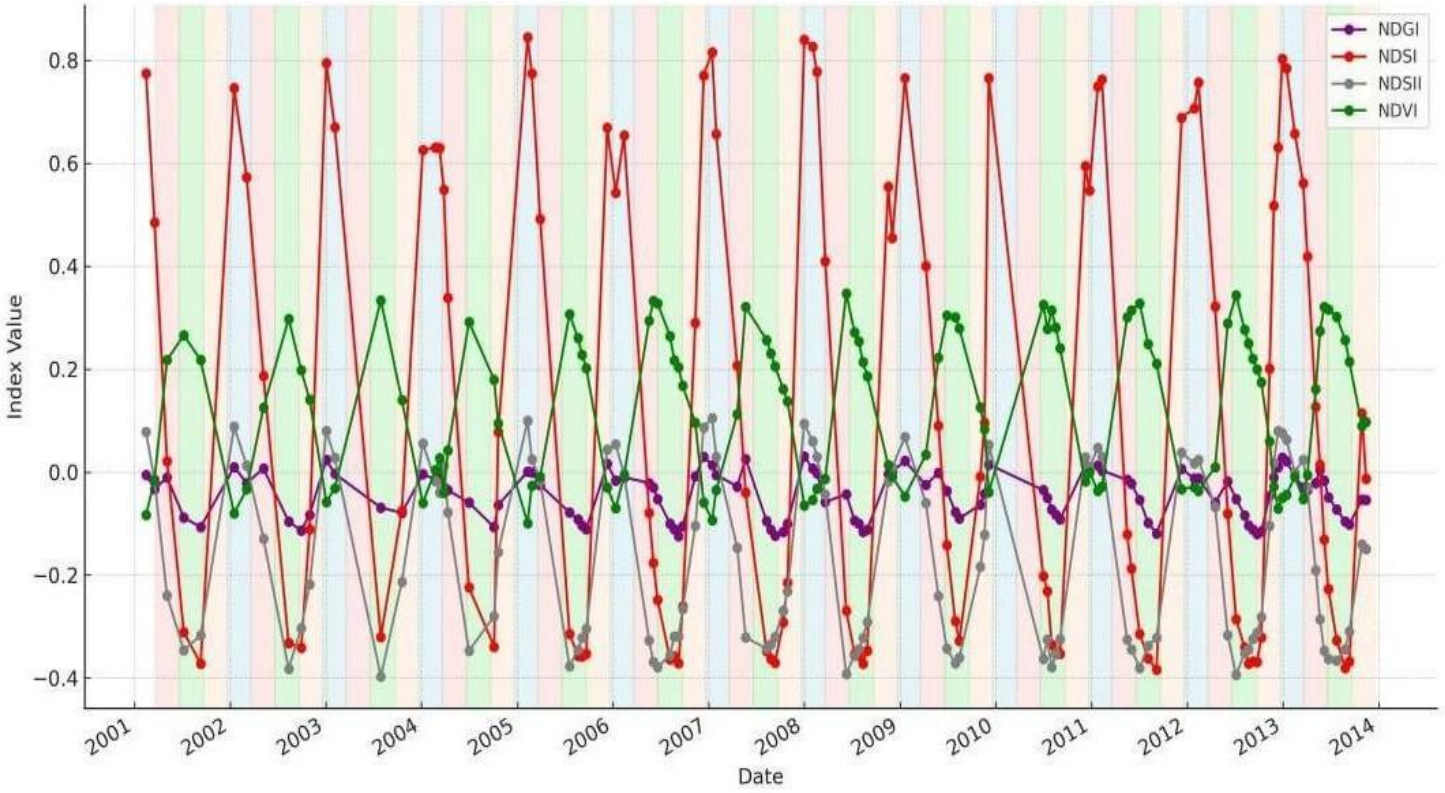

Figure 5. Time-series analysis of the cryosphere of Bostonliq district from 2001 to 2014 using Landsat 7 ETM.

Within the Bostonliq district, the interannual and seasonal dynamics of environmental indices, as observed through Landsat 8 OLI data for the period of 2014–2022, revealed distinct patterns over the course of several years (Figure 6). The NDVI, reflecting vegetation vigour, consistently climbed during the warm growing seasons of spring and summer, only to fall as the cold seasons of autumn and winter set in. This ebb and flow of greenery captured over successive years underscores the phenological responses of the area to seasonal temperature shifts. Conversely, the NDSI, which highlights snow presence, surges in the winter months, marking the landscape with a blanket of snow that recedes with warmer spring temperatures. The slight annual variations in the NDGI indicate the relative stability of glaciers, with minor seasonal alterations potentially linked to snow deposition rather than to changes in the ice itself.

NDSII shows the complex interplay between snow and ice surfaces, further dissecting the winter snowy cloak to reveal the underlying ice. Over the observed period, these indices together sketch a cyclical natural tapestry of the Bostonliq district, characterised by the rhythmic greening of vegetation, winter whitening of snow, and persistent, though subtly varying, glacial landscape, offering a nuanced view of the district's ecological cadence and climatic resilience.

The correlation matrix for the Bostonliq district showed intricate relationships between various environmental indices and climatic factors over the observed period. The mean NDVI, indicative of vegetation vitality, displayed a strong positive correlation with the monthly mean air temperature (0.91) and soil temperature (0.92), confirming the role of warmth in fostering plant growth.

Conversely, its negative correlation with precipitation (-0.44) suggests that increased rainfall does not align with vegetative proliferation, perhaps because of oversaturation or unfavourable timing of precipitation events (Figure 7).

Similarly, the NDSI mean, a measure of snow cover, was inversely correlated with the monthly mean air temperature (-0.91) and soil temperature (-0.91), reflecting the expected melting of snow with rising temperatures. Notably, NDSI was positively correlated with precipitation (0.53), implying that higher precipitation could be associated with snow accumulation during colder periods.

The NDGI mean, which reflects glacier extent and is positively correlated with the NDSI mean (0.83), indicates a possible link between snow coverage and glacial areas. The negative correlations with air monthly mean temperature (-0.57) and soil temperature (-0.61) were less intense, suggesting a more nuanced response of glaciers to temperature changes compared to snow cover.

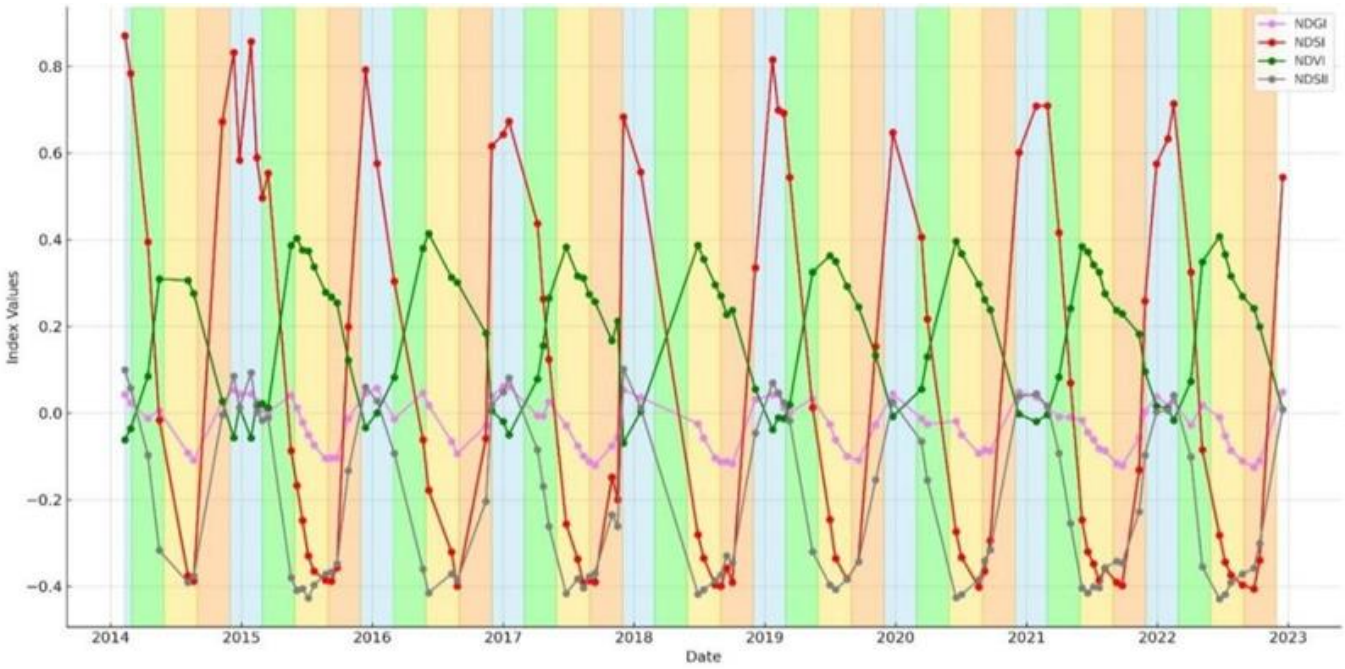

Figure 6. Time-series analysis of the cryosphere of Bostonliq district from 2014-2022 using Landsat 8 OLI.

Finally, the mean NDSII, which differentiates snow from ice, showed a strong positive correlation with the mean NDSI (0.94), underscoring their related but distinct responses to climatic conditions. It also exhibited significant negative correlations with both the monthly mean air temperature (-0.98) and soil temperature (-0.94), emphasizing the susceptibility of snow and ice to warmer temperatures.

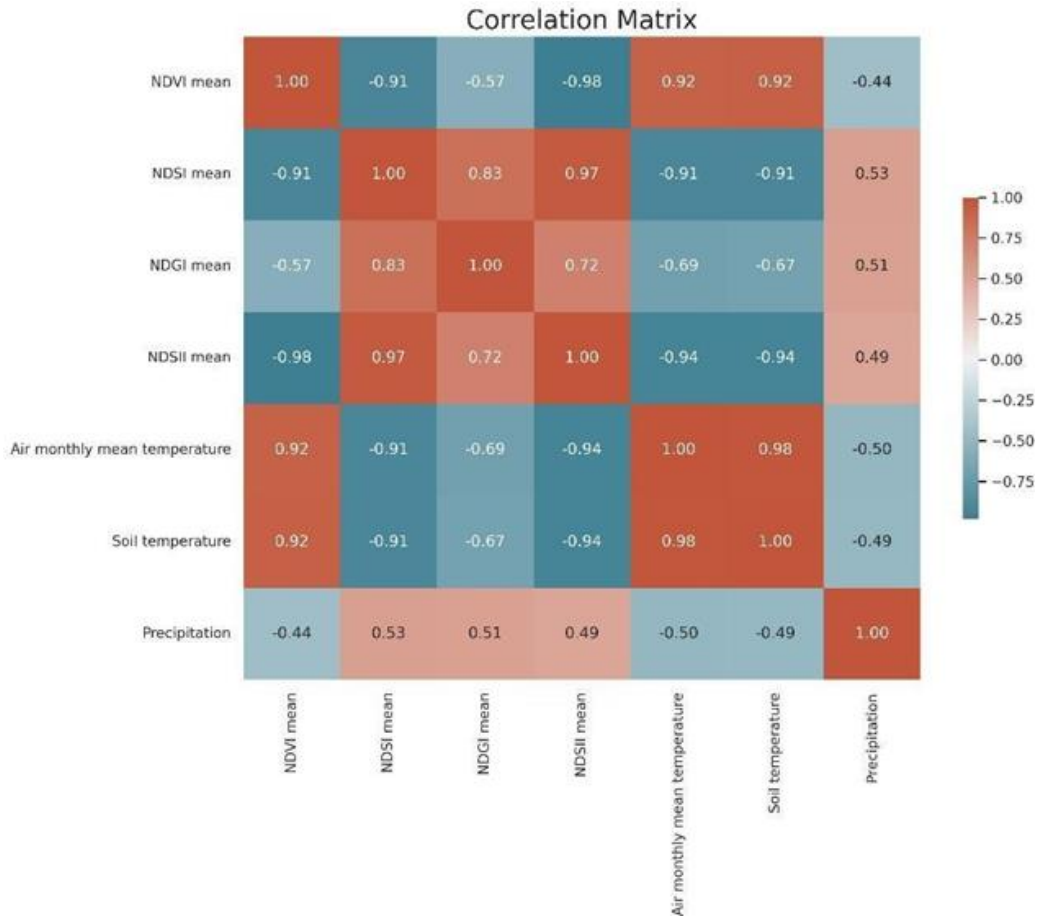

Figure 7. Linear relationship between mean values.

This matrix not only reflects the expected trends, such as the inverse relationship between temperature and snow indices but also captures subtle interactions, such as the negative relationship between vegetation and precipitation. These correlations offer a detailed view of the interplay between climate and the environment in the Bostonliq District, providing valuable data for ecological and climatic analyses.

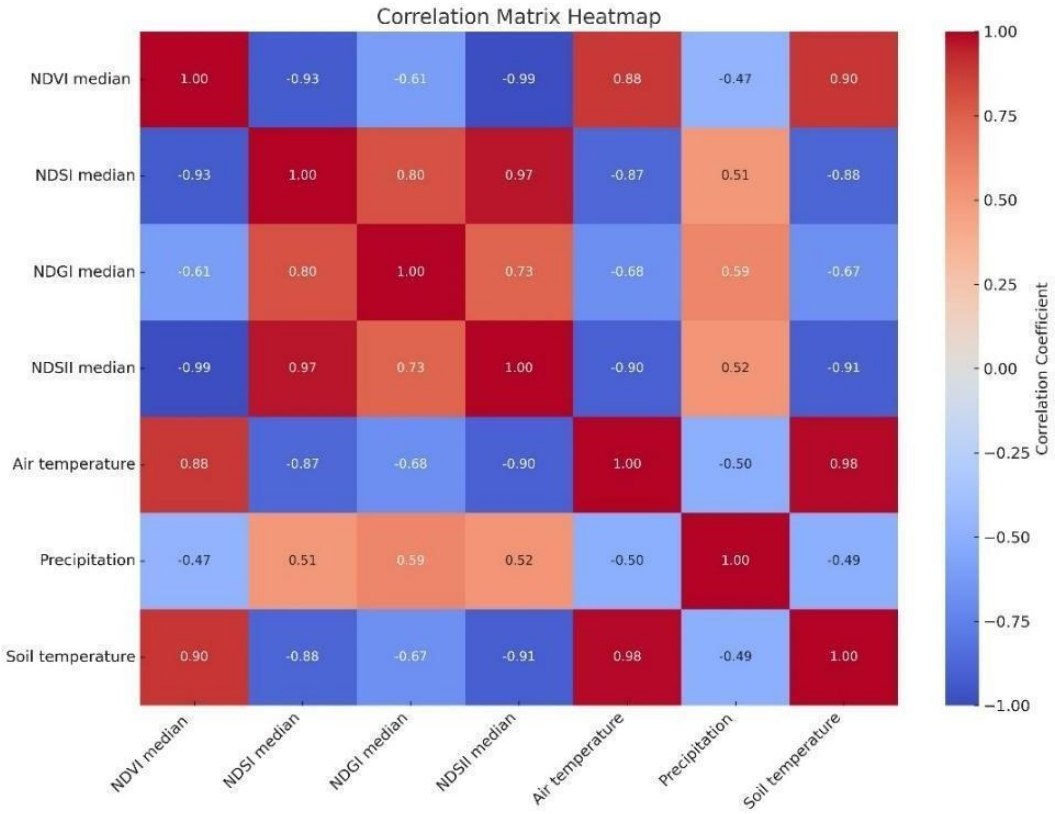

Figure 8. Linear relationships between median values.

The correlation matrix heatmap for the Bostonliq district (Figure 8), represented by blue and red shades, visualises the strength of the relationships between the environmental indices and climatic variables. The significant positive correlation between the median NDVI and air temperature (0.93) aligns with the understanding that warmer air fosters plant growth. A moderate positive correlation with soil temperature (0.47) and a weak negative correlation with precipitation (-0.43) is also observed, suggesting that vegetation health is more sensitive to air temperature changes than soil temperature or precipitation in this region.

The NDSI median, which detects snow cover, showed a strong negative correlation with the mean monthly air temperature (-0.93) and a moderate negative correlation with the mean monthly soil temperature (-0.52), confirming that snow presence diminishes with increasing temperatures. It had a moderately positive correlation with precipitation (0.51), indicating that higher precipitation may lead to increased snowfall during colder periods.

The NDGI median exhibited a strong negative correlation with mean air temperature (-0.80) and a moderate negative correlation with mean monthly soil temperature (-0.48), suggesting that glacial coverage declines as temperature rises. A moderate positive correlation with the NDSI median (0.73) implies that glaciers in the district might accumulate snowfall, thereby impacting their observed surface area.

Finally, the NDSII median, which differentiates snow from ice, had an extremely strong negative correlation with air temperature (-0.99), a moderate negative correlation with soil temperature (-0.52), and a moderate positive correlation with precipitation (0.52). This pattern highlights that snow and ice conditions are highly responsive to air temperature variations, less responsive to soil temperature variations, and are influenced by precipitation levels.

Overall, the heatmap underscores the inverse relationship between temperature and snow/ice-related indices, whereas vegetation shows a complex dependency on air and soil temperature. These findings underscore the district's ecological sensitivity to climatic variables and inform conservation and resource management strategies. For the NDSI, which measures snow cover, both mean (-0.91) and median (-0.93) show strong negative correlations with air temperature, again pointing to a consistent inverse relationship across the board. However, the median values had a slightly higher correlation with precipitation (0.51) than the mean (0.53), which could indicate that the median values may better represent the central tendency of the snow cover response to precipitation, possibly due to outliers in snowfall events.

Finally, the correlation of the NDSII with air temperature was almost identical and highly negative for both mean (-0.98) and median (-0.99) values, emphasizing a very consistent strong inverse relationship between air temperature and the differentiation between snow and ice, regardless of the measure of central tendency used.

In conclusion, while the median and mean correlations with air temperature were largely similar, suggesting robust trends, the discrepancies in the soil temperature and precipitation correlations indicate skewed distributions or the presence of outliers in the dataset. These differences highlight the importance of considering both mean and median values in environmental studies to capture a complete picture of the relationships between variables.

The series of graphs present the trend analysis for the NDSI mean, NDGI mean, and NDSII mean indices over a specified period, employing the MK test to statistically determine the presence of trends within the time-series data (Figures 9,10 and 11). Each graph was tailored to display the behaviour of the individual environmental index over time, with the data points represented as coloured dots and the trend highlighted by a distinctively coloured line. The analysis aimed to discern patterns and quantify the direction and magnitude of changes in these environmental indicators.

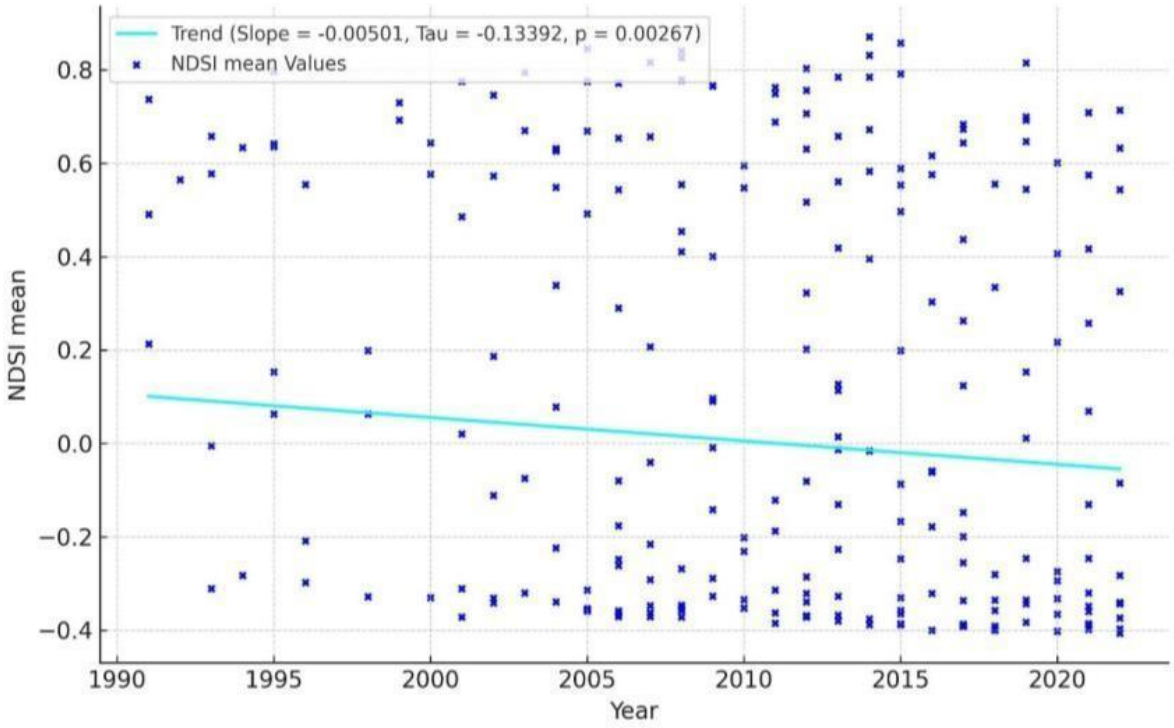

Figure 9. Snow index trend during the post-soviet period (1991–2022).

The NDSI mean graph (Figure 9) illustrates a negative trend over the observation period, indicated by a cyan trend line against the blue dots representing the actual data points. This trend suggests a gradual decrease in snow/ice cover or similar parameters as measured by the NDSI. The statistical measures provided in the graph's legend, including a negative Kendall Tau value, a significant p-value, and Sen's slope, reinforce confidence in the detected downward trend.

In contrast, the NDGI mean graph (Figure 10), with green dots and a lime trend line, shows a relatively flat trend, as evidenced by a near-zero Sen's Slope and a Kendall Tau value, which indicate a weak correlation. The high p-value further suggests that the observed trend was not statistically significant, implying that the NDGI, which may be related to greenness or vegetation health, remained relatively stable over the period analysed.

The NDSII mean graph (Figure 11) exhibits a negative trend, similar to the NDSI mean, with orange dots for the data points and a red line depicting the trend. This downward trend was statistically significant, as indicated by a negative Sen's slope and a positive but small Kendall's tau value, along with a very low p-value. This decline may reflect changes in environmental factors measured by the NDS II index, suggesting possible deterioration or alteration in the specific conditions it monitors.

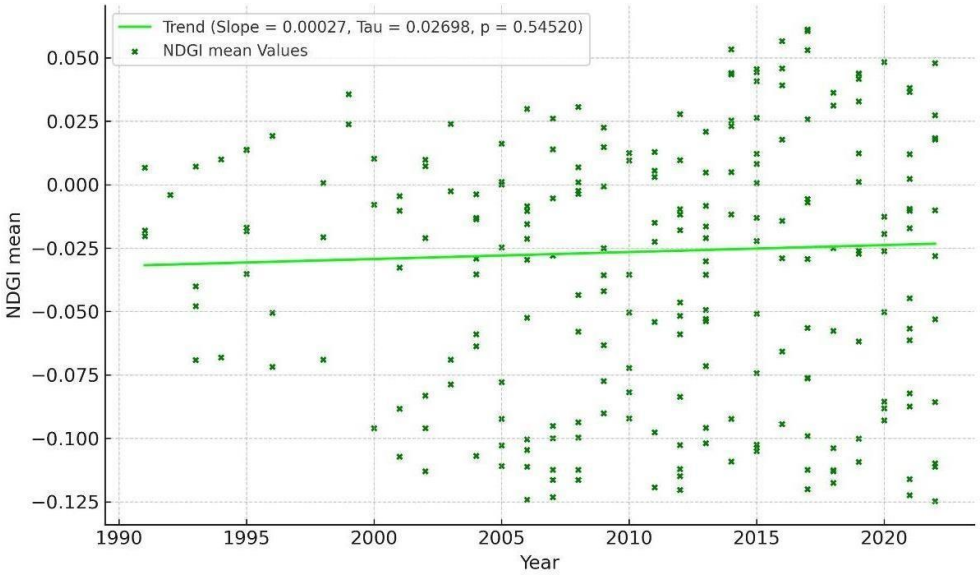

Figure 10. Glaciers index trend during the post-soviet period.

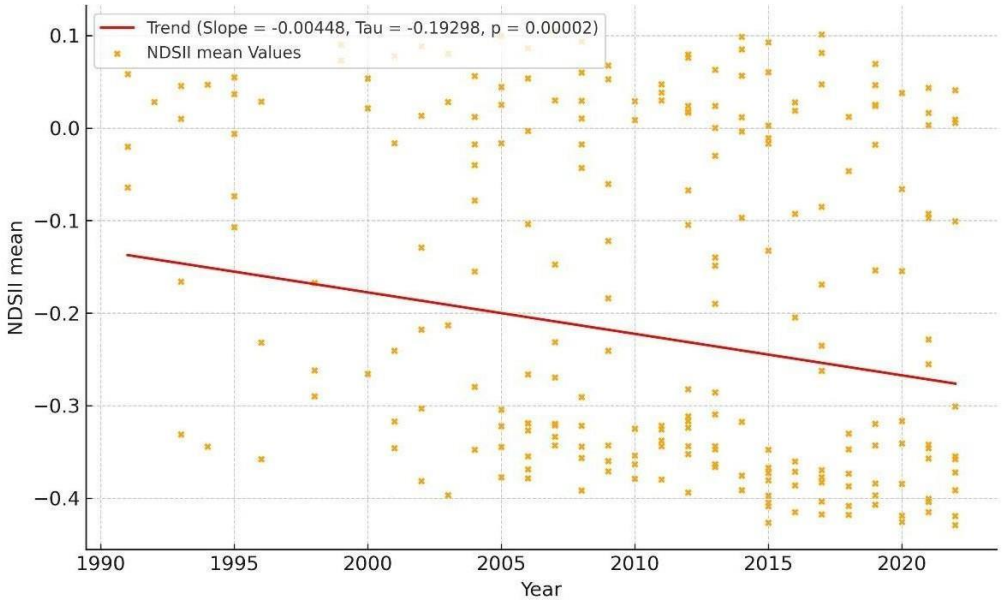

Figure 11. Snow-ice index trend during the post-soviet period.

As shown in Figure 4, there were many abruptions in the image dates during this period. A higher density and number of images would provide better clarity about the cryosphere change for the post-Soviet period and more accurate values of correlation between the cryosphere, vegetation, and climate variables.

Even though the MK test showed that the trend for glaciers is not statistically significant, many other studies have shown that glaciers in the Tian Shan Mountains have continued to diminish over the last 50–60 years. Many images for summer and autumn (when the glaciers have the smallest areas) are absent, which may indicate that the glaciers are actually increasing (as shown by the MK test in Figure 10). Nevertheless, observing only 20 years of the MK tests was insufficient to obtain robust findings. Therefore, other studies, especially those with field data of glacier observations, must be considered when making conclusions about the glacier state in the region.

The results of land use and land cover classification for the post-Soviet period for the Tashkent and Bostonliq districts unanimously claimed a decline in the cryosphere area (Alikhanov *et al.,* 2020; Alikhanov *et al.,* 2021; Juliev *et al*., 2019). Juliev's research for the study period 1989–2017 showed a slight decline—only several percent—in snow cover. In a study of Tashkent province from 1992 to 2018, the research showed a drastic decline in glacier, snow, and ice cover from 1800 km^2 in 1992 to 260 km^2. Nevertheless, the robustness of these results is questionable because the images were captured on different days of the year (Alikhanov *et al.,* 2020). However,

in a recent longitudinal study of the Bostanliq district, authors discovered an almost 30% decrease in the cryosphere (mainly, in snow cover at lower altitudes) during the post-Soviet period of time.

4. Conclusion

A comprehensive analysis of the cryosphere's response to climate change in Ugam Chatkal National Park, Uzbekistan, using remote sensing and statistical methods, revealed significant declining trends in the region's cryosphere conditions. The MK test and Sen's slope calculations applied to the NDSI, NDGI, NDVI, and NDSII indices highlighted observable changes in snow/ice cover, glacier extent, and the differentiation between snow and ice over the post-Soviet period. Trends indicate a decrease in snow and ice cover and alterations in glacier-related indices, reflecting the broader impacts of climate warming on the cryosphere of the region. These findings underscore the necessity for ongoing monitoring and adaptive management strategies to mitigate the effects of climate change on this sensitive ecosystem and ensure water security and ecological stability in Central Asia.

References

Alikhanov, B., Alikhanova, S., Oymatov, R., Fayzullaev, Z., & Pulatov, A. (2020). Land cover change in Tashkent province during 1992 – 2018. *IOP Conference Series: Materials Science and Engineering*, 883(1), 012088. doi: 10.1088/1757-899X/883/1/012088

Alikhanov, B., Juliev, M., Alikhanova, S., & Mondal, I. (2021). Assessment of influencing factor method for delineation of groundwater potential zones with geospatial techniques. Case study of Bostanlik district, Uzbekistan. *Groundwater for Sustainable Development,* 12, 100548. doi: 10.1016/j.gsd.2021.100548

Barandun, M., Fiddes, J., Scherler, M., Mathys, T., Saks, T., Petrakov, D., & Hoelzle, M. (2020). The state and future of the cryosphere in Central Asia. *Water Security*, 11, 100072. doi: 10.1016/j.wasec.2020.100072

Choubin, B., Heydari Alamdarloo, E., Mosavi, A., Sajedi Hosseini, F., Ahmad, S., Goodarzi, M., & Shamshirband, S. (2019). Spatiotemporal dynamics assessment of snow cover to infer snowline elevation mobility in the mountainous regions. *Cold Regions Science and Technology*, 167, 102870. doi: 10.1016/j.coldregions.2019.102870

Diebold, A. (2013). The impact of glaciers melting on national and trans-boundary water systems in Central Asia [Seminar report].

Florath, J., Keller, S., Abarca-del-Rio, R., Hinz, S., Staub, G., & Weinmann, M. (2022). Glacier Monitoring Based on Multi-Spectral and Multi-Temporal Satellite Data: A Case Study for Classification with Respect to Different Snow and Ice Types. *Remote Sensing*, 14(4), 845. doi: 10.3390/rs14040845

Frolov, D. M., Koshurnikov, A. V., Gagarin, V. E., Dodoboev, E. I., & Nabiev, I. A. (2023). Modern studies of the cryosphere of the Zeravshan and Gissar Ranges (Tien Shan). *E3S Web of Conferences*, 411, 02053. doi: 10.1051/e3sconf/202341102053

Gabban, A., Liberta, G., San-Miguel-Ayanz, J., & Barbosa, P. (2004). Forest fire risk estimation from time series analisys of NOAA NDVI data. *SPIE Digital Library*, 5232, 1-9. doi: 10.1117/12.511003

Gardner, A. S., Moholdt, G., Cogley, J. G., Wouters, B., Arendt, A. A., Wahr, J., Berthier, E., Hock, R., Pfeffer, W. T., Kaser, G., Ligtenberg, S. R. M., Bolch, T., Sharp, M. J., Hagen, J. O., Van Den Broeke, M. R., & Paul, F. (2013). A Reconciled Estimate of Glacier Contributions to Sea Level Rise: 2003 to 2009. *Science*, 340(6134), 852–857. doi: 10.1126/science.1234532

Gascoin, S., Barrou Dumont, Z., Deschamps-Berger, C., Marti, F., Salgues, G., López-Moreno, J. I., Revuelto, J., Michon, T., Schattan, P., & Hagolle, O. (2020). Estimating Fractional Snow Cover in Open Terrain from Sentinel-2 Using the Normalized Difference Snow Index. *Remote Sensing*, 12(18), 2904. doi: 10.3390/rs12182904

Gul, J., Muhammad, S., Liu, S., Ullah, S., Ahmad, S., Hayat, H., & Tahir, A. A. (2020). Spatio-temporal changes in the six major glaciers of the Chitral River basin (Hindukush Region of Pakistan) between 2001 and 2018. *Journal of Mountain Science*, 17(3), 572–587. doi: 10.1007/s11629-019-5728-9

Haeberli, W. (2004). Glaciers and ice caps: Historical background and strategies of worldwide monitoring. In J. L. Bamber & A. J. Payne (Eds.), Mass Balance of the Cryosphere. *Cambridge University Press*, 1, 559–578. doi: 10.1017/CBO9780511535659.017

Hall, D. K., & Riggs, G. A. (2011). Normalized-Difference Snow Index (NDSI). In V. P. Singh, P. Singh, & U. K. Haritashya (Eds.), Encyclopedia of Snow, Ice and Glaciers. *Springer Netherlands*, 779–780. doi: 10.1007/978-90-481-2642-2_376

Hall, D. K., Riggs, G. A., & Salomonson, V. V. (1995). Development of methods for mapping global snow cover using moderate resolution imaging spectroradiometer data. *Remote Sensing of Environment*, 54(2), 127–140. doi: 10.1016/0034-4257(95)00137-P

He, Q., Zhang, Z., Ma, G., & Wu, J. (2020). Glacier Identification From Landsat8 Oli Imagery Using Deep U-Net. Isprs Annals of the Photogrammetry. *Remote Sensing and Spatial Information Sciences*, 3, 381–386. doi: 10.5194/isprs-annals-V-3-2020-381-2020

Hill, E. A., Carr, J. R., & Stokes, C. R. (2017). A Review of Recent Changes in Major Marine-Terminating Outlet Glaciers in Northern Greenland. *Frontiers in Earth Science*, 4, 111. doi: 10.3389/feart.2016.00111

Hussien, K., Kebede, A., Mekuriaw, A., Beza, S. A., & Erena, S. H. (2023). Spatiotemporal trends of NDVI and its response to climate variability in the Abbay River Basin, Ethiopia. *Heliyon*, 9(3), e14113. doi: 10.1016/j.heliyon.2023.e14113

Juliev, M., Pulatov, A., Fuchs, S., & Hübl, J. (2019). Analysis of Land Use Land Cover Change Detection of Bostanlik District, Uzbekistan. *Polish Journal of Environmental Studies*, 28(5), 3235–3242. doi: 10.15244/pjoes/94216

Kenner, R., Noetzli, J., Hoelzle, M., Raetzo, H., & Phillips, M. (2019). Distinguishing ice-rich and ice-poor permafrost to map ground temperatures and ground ice occurrence in the Swiss Alps. *The Cryosphere*, 13(7), 1925–1941. doi: 10.5194/tc-13-1925-2019

Keshri, A. K., Shukla, A., & Gupta, R. P. (2009). ASTER ratio indices for supraglacial terrain mapping. International *Journal of Remote Sensing*, 30(2), 519–524. doi: 10.1080/01431160802385459

Mann, H. B. (1945). Nonparametric Tests Against Trend. *Econometrica*, 13(3), 245. doi: 10.2307/1907187

Acknowledgements

Acknowledgements can be delivered to the parties who have helped research and completion of the writ- ing of the manuscript. These parties can act as mentors, funders, provid- ers of data, and so forth.

Author Contributions

Conceptualization: Alikhanov, B., Pulatov, B.; **methodology:** Alikhanov, B., Pulatov, B.; **investigation:** Alikhanov, B.; **writing—original draft preparation:** Alikhanov, B., Samiev, L.; **writing—review and editing:** Alikhanov, B., Pulatov, B., & Samiev, L.; **visualization:** Alikhanov, B., Pulatov, B., & Samiev, L. All authors have read and agreed to the published version of the manuscript.

Conflict of interest

All authors declare that they have no conflicts of interest.

Data availability

Data is available upon Request.

Funding

This research received no external funding.

Mohammadi, B., Pilesjö, P., & Duan, Z. (2023). The superiority of the Adjusted Normalized Difference Snow Index (ANDSI) for mapping glaciers using Sentinel-2 multispectral satellite imagery. *GIScience & Remote Sensing*, 60(1), 2257978. doi: 10.1080/15481603.2023.2257978

NSIDC. (2024). *National Snow and Ice Data Center*. Retrived from https://nsidc.org/

Nüsser, M. (2017). Socio-hydrology: A New Perspective on Mountain Waterscapes at the Nexus of Natural and Social Processes. Mountain Research and Development, 37(4), 518–520. doi: 10.1659/MRD-JOURNAL-D-17-00101.1 Parajka, J., Pepe, M., Rampini, A., Rossi, S., & Blöschl, G. (2010). A regional snow-line method for estimating snow cover from MODIS during cloud cover. *Journal of Hydrology*, 381(3–4), 203–212. doi: 10.1016/j.jhydrol.2009.11.042

Petrov, M. A., Sabitov, T. Y., Tomashevskaya, I. G., Glazirin, G. E., Chernomorets, S. S., Savernyuk, E. A., Tutubalina, O. V., Petrakov, D. A., Sokolov, L. S., Dokukin, M. D., Mountrakis, G., Ruiz-Villanueva, V., & Stoffel, M. (2017). Glacial lake inventory and lake outburst potential in Uzbekistan. *Science of The Total Environment*, 592, 228–242. doi: 10.1016/j.scitotenv.2017.03.068

Robson, B. A., Bolch, T., MacDonell, S., Hölbling, D., Rastner, P., & Schaffer, N. (2020). Automated detection of rock glaciers using deep learning and object-based image analysis. *Remote Sensing of Environment*, 250, 112033. doi: 10.1016/j.rse.2020.112033

Sen, P. K. (1968). Estimates of the Regression Coefficient Based on Kendall's Tau. *Journal of the American Statistical Association*, 63(324), 1379–1389. doi: 10.1080/01621459.1968.10480934

Shahgedanova, M., Afzal, M., Severskiy, I., Usmanova, Z., Saidaliyeva, Z., Kapitsa, V., Kasatkin, N., & Dolgikh, S. (2018). Changes in the mountain river discharge in the northern Tien Shan since the mid-20th Century: Results from the analysis of a homogeneous daily streamflow data set from seven catchments. *Journal of Hydrology*, 564, 1133–1152. doi: 10.1016/j.jhydrol.2018.08.001

Singh, V. P., Singh, P., & Haritashya, U. K. (2011). Encyclopedia of Snow, Ice and Glaciers. *Springer Netherlands*.

Sood, V., Singh, S., Taloor, A. K., Prashar, S., & Kaur, R. (2020). Monitoring and mapping of snow cover variability using topographically derived NDSI model over north Indian Himalayas during the period 2008–19. *Applied Computing and Geosciences*, 8, 100040. doi: 10.1016/j.acags.2020.100040

Sorg, A., Kääb, A., Roesch, A., Bigler, C., & Stoffel, M. (2015). Contrasting responses of Central Asian rock glaciers to global warming. *Scientific Reports*, 5(1), 8228. doi: 10.1038/srep08228

Stoffel, M., & Huggel, C. (2012). Effects of climate change on mass movements in mountain environments. *Progress in Physical Geography: Earth and Environment,* 36(3), 421–439. doi: 10.1177/0309133312441010

Velicogna, I., & Wahr, J. (2013). Time-variable gravity observations of ice sheet mass balance: Precision and limitations of the GRACE satellite data. *Geophysical Research Letters*, 40(12), 3055–3063. doi: 10.1002/grl.50527

Wang, H., Yang, R., Li, X., & Cao, S. (2017). Glacier parameter extraction using Landsat 8 images in the eastern Karakorum. *IOP Conference Series: Earth and Environmental Science*, 57, 012004. doi: 10.1088/1755-1315/57/1/012004

Worni, R., Huggel, C., Clague, J. J., Schaub, Y., & Stoffel, M. (2014). Coupling glacial lake impact, dam breach, and flood processes: A modeling perspective. *Geomorphology*, 224, 161–176. doi: 10.1016/j.geomorph.2014.06.031

Xiong, Q., Wang, Y., Liu, D., Ye, S., Du, Z., Liu, W., Huang, J., Su, W., Zhu, D., Yao, X., & Zhang, X. (2020). A Cloud Detection Approach Based on Hybrid Multispectral Features with Dynamic Thresholds for GF-1 Remote Sensing Images. *Remote Sensing*, 12(3), 450. doi: 10.3390/rs12030450

Zhang, G., Yao, T., Xie, H., Kang, S., & Lei, Y. (2013). Increased mass over the Tibetan Plateau: From lakes or glaciers?. *Geophysical Research Letters*, 40(10), 2125–2130. doi: 10.1002/grl.50462